Journal of the Chinese Chemical Society, **1998**, *45*, 701-706

Synthesis, Crystal Structure, Cryomagnetic Properties and Catalytic Activity for H_2O_2 Disproportionation of New Dinuclear and Polynuclear Bis(2,4-pentanedionate)manganese(II) Complexes with Diazine Ligands

D. M. Hong*[a] (洪當明), H. H. Wei*[b] (魏和祥), K. H. Chang[b] (張國輝), G. H. Lee[c] (李錦祥) and Yu Wang[c] (王 瑜)

[a]*Tzu-Chi Junior College of Nursing, Hualien, Taiwan, R.O.C.*

[b]*Department of Chemistry, Tamkang University, Tamsui, Taiwan, R.O.C.*

[c]*Instrumentation Center, College of Science, National Taiwan University, Taipei, Taiwan, R.O.C.*

The structures, magnetic properties, and catalytic activity for H_2O_2 disproportionation are reported for three new complexes $[Mn_2(acac)_4(pydz)]$ (**1**), $[Mn(acac)_2(pym)]$ (**2**), and $[Mn(acac)_2(pyz)]$ (**3**) (acac= 2,4-pentanedionate, pydz = pyridazine, pym = pyrimidine, pyz = pyrazine). The X-ray crystal structures of **1** and **3** have been determined. Complex **1** crystallizes as a binuclear complex with η^2-pyridazine and acac bridging ligands **3** crystallizes as a linear polymeric chain with bridging pyrazine molecule. Cryomagnetic investigations (4-300 K) reveal a weak intramolecular antiferromagnetic spin exchange with J = -2.05, -0.04, and -0.05 cm^{-1} for the complexes of **1**, **2**, and **3**, respectively. The complexes **1-3** showed two-step catalytic activity for H_2O_2 disproportionation in pyridine solution at 0 °C.

INTRODUCTION

Multinuclear manganese cores play indispensable roles in biologically important manganese redox enzymes[1] involved in the oxygen-evolving complexes of photosystem II of green plants[1-2] and catalases.[1,3] It has been pointed out that X-ray structure analysis of the manganese catalase from *thermus thermophilus* revealed the two manganese ions are separated by 3.3 Å.[1] A similar catalase-like active center was observed in the photosynthetic system of water oxidation enzyme, which has a tetranuclear manganese cluster with 2.7-3.3 Å of Mn-Mn distances.[4] Therefore, the intermetallic separation and the arrangement of proximal ligands are essential in the design of O_2-evolving model manganese complexes. Recently, binuclear manganese(II/II) complexes have been proposed as structural models of the dimanganese catalase-like enzymes.[5]

Heterocyclic diazines such as pyrazine, pyrimidine, and pyridazine are known to be an excellent bridging ligand when coordinated to transition metals.[6-7] Binuclear metal complexes bridged by pyridazine are of particular interest because this bridge ligand provides a shorter metal-metal separation of 3.2-4.5 Å relevant to bimetallic enzymes. However, only a few reports deal with manganese(II) complexes with diazine ligands.[7] In our laboratory, we have prepared three new manganese(II) complexes of $[Mn_2(acac)_4(pydz)]$ (**1**), $[Mn(acac)_2(pym)]$ (**2**), and $[Mn(acac)_2(pyz)]$ (**3**), (acac = 2,4-pentanedionate, pydz = pyridazine, pym = pyrimidine and pyz = pyrazine). In this paper we report on the synthesis, X-ray crystal structure, cryomagnetic property and catalase activity investigations of complexes **1**, **2**, and **3**.

EXPERIMENTAL

Synthesis of Complexes

Bis(2,4-pentanedionate)manganese(II), $[Mn(acac)_2]\cdot 2H_2O$, was prepared from the metal acetate by a standard procedure.[8] Pyridazine (pydz), pyrimidine (pym), and pyrazine (pyz) were purchased from a commercial source (Aldrich Chemical Co.) and used without further purification.

$[Mn_2(acac)_4(pydz)]$ (**1**), $[Mn(acac)_2(pym)]$ (**2**), and $[Mn(acac)_2(pyz)]$ (**3**) were synthesized by mixing an absolute ethanol solution of the complex $[Mn(acac)_2]\cdot 2H_2O$ and an ethanolic solution of an equimolar quantity of diazines. After standing for a few days, light-brown crystals of **1** (80% yield), light-yellow crystals of **2** (85% yield) and **3** (80% yield) were filtered off, air dried and characterized initially by elemental analysis, IR, and also by single-crystal X-ray diffractional analysis for **1** and **3**. Anal. Calc for $C_{24}H_{32}N_2Mn_2O_8$ (**1**): C, 49.2; H, 5.5. N, 4.9. Found: C, 48.8; H, 5.4; N, 4.8%. Calc for $C_{14}H_{18}N_2MnO_4$ (**2**): C, 50.5; H, 5.4; N, 8.4. Found: C, 50.6; H, 5.4; N, 8.4%. Calc for $C_{14}H_{18}N_2MnO_4$ (**3**): C, 50.5; H, 5.4; N, 8.4%. Found: C,

50.5; H, 5.5; N, 8.5%.

X-ray Structure Determination Crystallography

Crystallographic data for the complexes **1** and **3** were collected on an Enraf-Nonius CAD-4 diffractometer with graphite-monochromatized Mo-K_α radiation (λ = 0.7107 Å) at 25 °C. Crystallographic parameters and pertinent refinement results are summarized in Table 1. The structures were solved by the heavy-atom method and subsequent difference-Fourier maps followed by full-matrix least-squares based on F refinement with the NRCVAX computer program.[9] The function minimized was $\Sigma(|F_o|-|F_c|)^2$ and unit weights were used. All non-hydrogen atoms were readily located and refined with anisotropic thermal parameters; $R = \Sigma||F_o|-|F_c||/\Sigma|F_o|$ and $R_w = (\Sigma w(|F_o|-|F_c|)^2/\Sigma w|F_o|^2)^{1/2}$. The ORTEP plots of the molecules of **1** and **3** are shown in Figs. 1 and 2, respectively. Selected interatomic distances and angles are listed in Tables 2 and 3 for **1** and **3**, respectively. Complete crystal data, atomic positional parameters, and components of the anisotropic temperature factors are deposited as supplementary material.

Physical Measurements

IR spectra were recorded on a Bio-Rad FTS40 FTIR spectrophotometer as KBr pellets in the 4000-400 cm^{-1} region. X-band EPR spectra at 25 °C for the complexes in powder were recorded on a Bruker ESC-106 spectrometer. Temperature dependence of magnetic susceptibilities of the polycrystalline samples were measured between 4 and 300 K at a field 1 T using a Quantum Design Model MPMS computer-controlled SQUID magnetometer. Corrections for the diamagnetism of complexes were estimated from Pascal's constants.[10]

H_2O_2 Disproportionation Measurements

A closed vessel containing a pyridine solution (2 cm^3) of the manganese(II) complex **1** (1.5×10^{-5} mol) or complexs of **2** and **3** (3.0×10^{-5} mol) was stirred and kept at 25 °C. Hydrogen peroxide (35%, 2 cm^3, 20.6 mmol) was injected through the septum with a syringe. The reactor was connected to a graduated volumetric burette filled with water, and dioxygen evolution was measured at time intervals (during 5 and 10 s.) by volumetry.

RESULTS AND DISCUSSION

IR Spectra

The infrared spectra of complexes **1-3** display an intense absorption located in the 1617-1610 cm^{-1} range and at-

Table 1. Crystallographic Data for **1** and **3**

	1	**3**
Formula	$C_{24}H_{32}N_2Mn_2O_8$	$C_{14}H_{18}N_2MnO_4$
M	586.40	333.24
Crystal systm	Orthorhombic	Triclinic
Space group	P bcn	$P\bar{1}$
a/Å	14.356(4)	6.2695(24)
b/Å	8.6047(14)	6.272(4)
c/Å	22.535(6)	11.028(3)
α/°		93.50(3)
β/°		103.55(3)
γ/°		106.87(4)
U/Å^3	2783.8(12)	399.5(3)
Z	4	1
D_c/g cm^{-3}	1.399	1.385
λ/Å	0.7107	0.7107
μ/cm^{-1}	9.152	8.074
Crystal size/mm	0.25 × 0.25 × 0.30	0.05 × 0.20 × 0.30
Temperature/K	298	298
No. of reflections measured	2442	1423
No. of reflections observed	1296	1083
R	0.037	0.060
R_w	0.036	0.059
GoF	1.51	2.07
$(\delta/\sigma)_{max}$	0.0009	0.0017

tributed to the CO group's stretching frequency of the acac ligand. In accordance with many IR spectra data concerning the transition metal complexes of acetylacetonate,[11] the absorptions observed at 1615, 1616, and 1617 cm^{-1} for compounds **1-3**, respectively, are attributed to CO stretching vibration of the coordinated carbonyls of the acac entity, while an additional medium absorption band at 1610 cm^{-1} for **1** is assigned to CO stretching vibration of the bridged carbonyl group of the acac moiety.

Description of the Crystal Structures

The crystal structure of the complex $[Mn_2(acac)_4(pydz)]$ **1** consists of the packing of discrete neutral binuclear molecules. The coordination geometry of manganese and the atom numbering scheme in **1** are shown in Fig. 1. The two metal ions are symmetrically bridged by one η^2-pydz ligand and by oxygen atoms(O(4)) of two acac ligands with a Mn···Mn′ separation of 3.3553(14) Å. The geometrical environment about each Mn is regarded as a distorted octahedral $MnNO_5$ chromophore with five acac oxygens and one nitrogen of the pydz ligand. The axial Mn-N bond distance 2.321(3) Å is longer than the 2.096(3) Å of Mn-O(1). The averaged bond distances for the oxygen-bridged Mn-O(4) (2.215 Å) are somewhat longer than the averaged bond distance of the chelated Mn-O (2.112 Å).

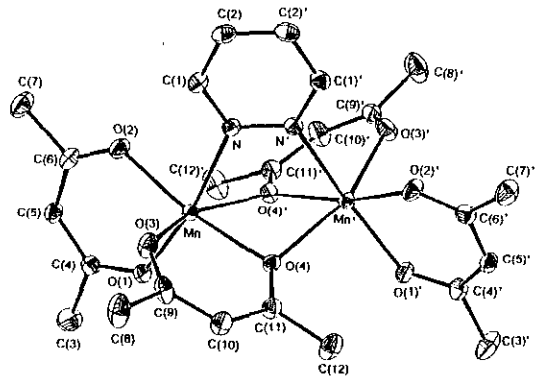

Fig. 1. ORTEP stereoview of $[Mn_2(acac)_4(pydz)]$ (**1**) with number scheme and vibrational ellipsoids at 30% probability level.

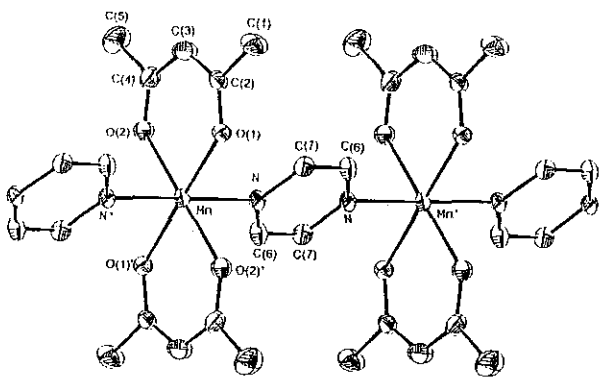

Fig. 2. ORTEP stereoview of $[Mn(acac)_2(pyz)]$ (**3**) with number scheme and vibrational ellipsoids at 30% probability level.

Table 2. Selected Bond Distances (Å) and Angles (°) for **1**

Mn-O(1)	2.096(3)	Mn-O(2)	2.111(3)
Mn-O(3)	2.130(3)	Mn-O(4)	2.130(3)
Mn-O(4)	2.240(3)	Mn-N	2.321(14)
N-N′	1.332(6)	Mn···Mn′	3.3553(14)
Mn-O(4)-Mn′	98.46(11)	O(1)-Mn-N	165.76(13)
O(2)-Mn-O(4)′	106.88(12)	O(2)-Mn-O(4)	167.24(12)
O(3)-Mn-O(4)	83.15(11)	O(3)-Mn-O(4)′	156.62(11)
Mn-N-N′	115.47(23)	O(4)-Mn-N	85.63(11)
O(4)-Mn-N	82.50(12)	O(4)-Mn-O(4)′	73.97(10)

The X-ray structural analysis of **3** revealed that the manganese(II) atom has an octahedral six-coordination (Fig. 2) MnN_2O_4 chromophore with four oxygen atoms (average Mn-O bond distance = 2.121 Å) of two acac ligands and two nitrogen atoms (Mn-N = 2.336(5) Å) of bridged pyz ligand. As a result, the Mn^{II} ions and the acac and pyz ligands form a one-dimensional polymeric chain structure (Fig. 2). The resulting Mn···Mn distance is 7.50 Å, much longer than that in complex **1**, resulting in a very weak magnetic interaction between the two Mn^{II} atoms.

EPR and Cryomagnetic Properties

The powder X-band EPR spectra (9.30 GHz) at 300 K of compounds **1-3** exhibit a ca. 850-900 G symmetrical broad resonances with g values of 2.00, 2.02 and 2.01 respectively. The broadness of these isotropic signals is consistent with polynuclear structures in which spin-spin relaxation is enhanced through large dipolar interactions mediated by the lattices of the solids.[12-13]

The temperature dependence of the molar magnetic susceptibility, χ_m and the magnetic moment, μ_{eff}, for **1**, **2**,

Table 3. Selected Bond Distances (Å) and Angles (°) for **3**

Mn-N	2.336(5)	Mn-O(1)	2.105(4)
Mn-O(2)	2.138(4)		
N-Mn-N′	179.9	O(1)-Mn-O(1)′	180.0
O(2)-Mn-O(2)′	180.0	O(1)-Mn-O(2)	84.53(14)
O(1)-Mn-N	89.89(15)	O(1)-Mn-N	90.11(15)
O(2)-Mn-N	89.91(16)	O(2)-Mn-N	90.09(16)
Mn-N-C(7)	121.7(4)	Mn-N-C(6)	122.6(4)

and **3** are depicted in Figs. 3, 4 and 5, respectively. The observed effective magnetic moment 7.85 μ_B at 300 K for **1** is lower than the non-coupled two spin state ($S_1 = 5/2$, $S_2 = 5/2$) value of 8.34 μ_B. As shown in Fig. 3, the molar susceptibility χ_m increases steadily with decreasing temperature, reaching a maximum at ca 30 K and then decreasing with decreasing temperature. The magnetic moment and temperature exhibits a continuous decrease upon cooling, with an extrapolated value that vanishes when T approaches zero. This behaviour is characteristic of an intramolecular antiferromagnetic interaction between two high-spin Mn^{II} ions through the η^2-pydz and acac-bridged ligands in $[Mn_2(acac)_4(pydz)]$ (**1**). The smooth solid curves of χ_m and μ_{eff} *versus* the T plots in Fig. 3 are a least-squares fit to the data using the Heisenberg-Dirac-Van-Vleck $S_1 = S_2 = 5/2$ isotropic spin-coupled model without zerofield splitting described in the equation (1).[14]

$$\chi_m = (Ng^2\mu_B{}^2/kT)(A/B) \quad (1)$$
$$A = 2e^{-x} + 10e^{-3x} + 28e^{-6x} + 60e^{-10x} + 110e^{-15x}$$
$$B = 1 + 3e^{-x} + 5e^{-3x} + 7e^{-6x} + 9e^{-10x} + 11e^{-15x}$$

where $x = 2J/kT$, N is Avogadro's number, μ_B is the Bohr magneton, k is Boltzman's constant. The values obtained for **1** are $J = -2.05$ cm^{-1}, $g = 2.00$, and $R = 5 \times 10^{-5}$, where R is the agreement factor defined as $\Sigma[(\chi_m)^{obs} - (\chi_m)^{calc}]^2/\Sigma[(\chi_m)^{obs}]^2$.

With no crystal structure at hand for complex **2**, we relied on IR and EPR spectroscopy to determine the most likely structural hypothesis able to account for the magnetic susceptibility results. The effective magnetic moments of **2** and **3** at 300 K are 5.89 and 5.94 μ_B, respectively, and are near the spin-only value of 5.90 μ_B usually observed for one high-spin Mn^{II} complex ($S = 5/2$). As shown in Fig. 4 and Fig. 5, the magnetic moments keep constant within the temperature 300 - 30 K region and then decrease with temperature, reaching a value of 5.66 μ_B for **2** and 5.74 μ_B for **3** at about 4 K. This behaviour is characteristic of a very weak

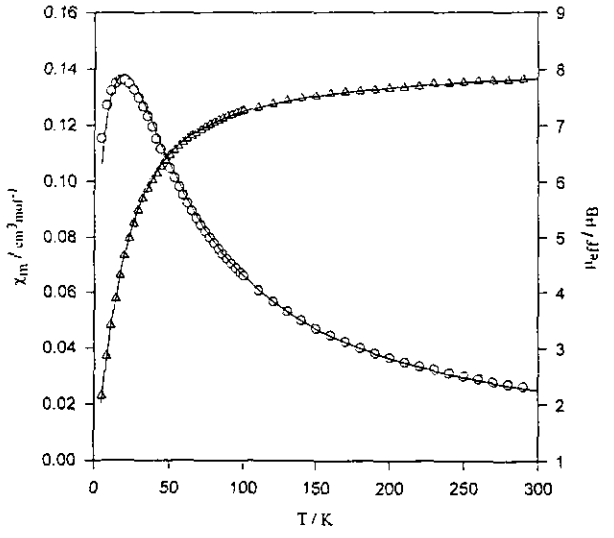

Fig. 3. Temperature dependences of χ_m (o) and μ_{eff} (Δ) of complex **1**. Solid lines represent the least-squares fit of the data to the equations (1) as given in the text.

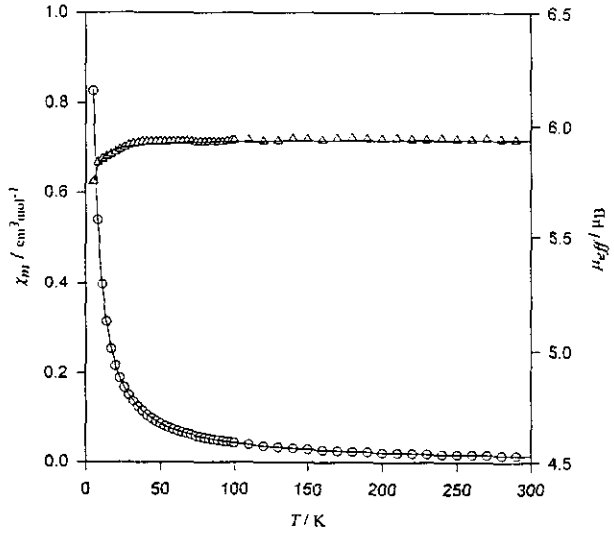

Fig. 4. Temperature dependences of χ_m (o) and μ_{eff} (Δ) of complex **2**. Solid lines represent the least-squares fit of the data to the equations (2) as given in the text.

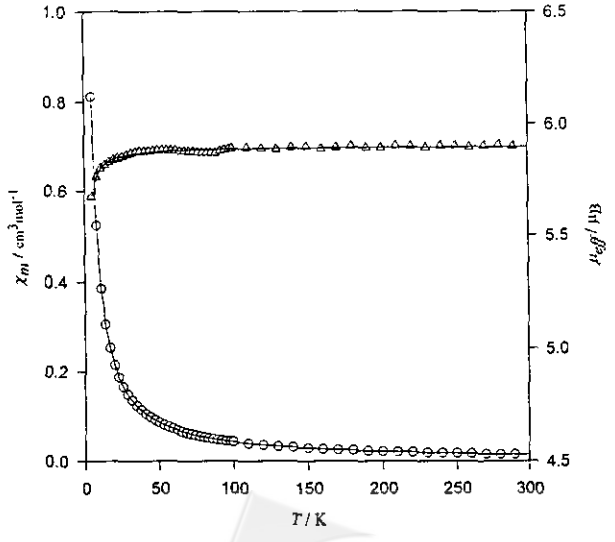

Fig. 5. Temperature dependences of χ_m (o) and μ_{eff} (Δ) of complex **3**. Solid lines represent the least-squares fit of the data to equation (2) as given in the text.

intra- or inter-chain antiferromagnetic interaction between two high-spin Mn^{II} ions through the pym and pyz bridge ligands in $[Mn(acac)_2(pym)]$ **2** and $[Mn(acac)_2(pyz)]$ **3** polymer chains. We have attempted to reproduce theoretically the experimental susceptibilities in these two one-dimensional complexes **2** and **3** by using one of the expressions calculated by Fischer for a classical-spin Heisenberg chain[10,15] scaled to a real spin $S = 5/2$:

$$\chi m = [2Ng^2\mu_B{}^2S(S+1)/3kT](1-\nu)/(1+\nu) \quad (2)$$

where $\nu = -\coth K + 1/K$, $K = JS(S+1)/kT$, N, μ_B, and k have their usual meaning. A very close agreement with the experiment is obtained with $J = -0.04$ cm^{-1}, $g = 2.02$, $R = 4 \times 10^{-5}$ for **2** and $J = -0.05$ cm^{-1}, $g = 2.01$, $R = 5 \times 10^{-5}$ for **3**, demonstrating a very weak magnetic interaction. The fitted g values give good agreement with those of the EPR results. The calculated isotropic exchange energies, J values for **2** and **3**, lie lower, which compared well to the value of axial zero-field splitting (D).[16]

Let us consider now the small, essentially axial anisotropy that appears in the susceptibility in the low temperature for the present systems. The zero-field splitting for $S = 5/2$ systems is almost entirely due to magnetic dipole-dipole interaction between the Mn(II) ions.[17] The interaction can be approximately calculated from the simple expression $D = (-g^2\mu_B{}^2/R^3)$,[16-17] where R is the separation between two Mn(II) ions. Using the values of 3.35 Å for **1** and 7.50 Å for **3**, the zero-field splittings, $|D| = 0.04$ for **1** and 0.005 cm^{-1} for **3**, are obtained, but they are much lower than the isotropic spin exchange energies.

For compounds **2** and **3**, their antiferromagnetic interactions are much weaker than that of compound **1**, the intramolecular Mn···Mn′ separation of which is as short as 3.35 Å and involves the acac bridging. The self-assembly bridged acac ones are able to transmit magnetic super-exchange between manganese(II) ions. The intrachain Mn···Mn separation of **3** is about 7.50 Å larger and without acac bridging.

The J value of -2.05 cm^{-1} found in $[Mn_2(acac)_4(pydz)]$ can be compared with other $Mn^{II}Mn^{II}$ magnetic interactions with other bridge systems. It is smaller than the values (-3.0 ~ -18 cm^{-1}) measured for the acetato bridged binuclear complexes,[13] but larger than the values (-0.15 ~ -1.50 cm^{-1}) obtained for croconto and oxalato-bridged binuclear Mn^{II} complexes.[12]

Catalytic Activity for H_2O_2 Disproportationation of 1, 2, and 3 Complexes

All complexes **1-3** showed catalytic activity for disproportionation of H_2O_2 in pyridine at O °C. The complexes **1-3** are ones with low catalase activity in CH_3OH or aqueous solution without base-addition that did decomposed H_2O_2 very slowly; it was found that the presence of added pryidine base was an extremely active conbination for H_2O_2-disproportionation. Besides, it was found that addition of pyridine only to the aqueous or methanol solution of complexes **1-3** without addition of H_2O_2 subtrate resulted in no O_2 evolving.

The time courses of the O_2-evolution are shown in Fig. 6. The initial O_2-evolution was rapid. Then after a lag period the rate significantly increased again. In the present case of complexes **1-3**, this dramatically shows two steps of H_2O_2-disproportionation. The insert shows the course of the volume of O_2-evolution with the initial time within 0-400 s. For the first 50 s, the turnover of H_2O_2-disproportionation of **1**, **2**, and **3** are 450, 110, and 150, respectively.

The above results show that addititon of the base pyridine causes a significant catalytic activity of complexes **1-3** toward H_2O_2-disproportionation. In this phenomenon the diazine base, weaker in donating ability than pyridine, is replaced with pyridine in complexes **1-3** to form a catalase-like catalyst. Earlier, it had been reported that the role of the base in H_2O_2-Mn catalase systems was to stabilize $Mn^{IV} = O$ intermediate complexes,[18] and it is also thought that the role of the added base to facilitate deprotonation of the H_2O_2 prior to its reaction with the manganese catalyst.[19] We are preparing further detailed studies on the kinetics, the cata-

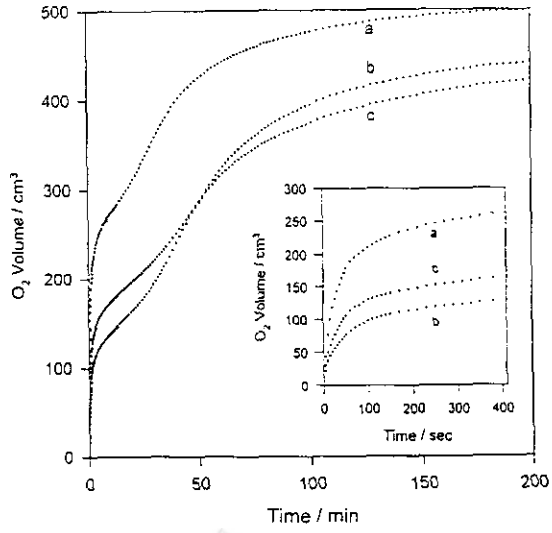

Fig. 6. Time course of O_2-evolution of H_2O_2 disproportionation by **1**(a), **2**(b), and **3**(c). *Conditions*: **1** (1.5×10^{-5} mol), **2** and **3** (3.0×10^{-5} mol) in pyridine (2 cm^3), H_2O_2 (35%, 2 cm^3, 20.6 mmol), at 25 °C.

lytic mechanism, and the characterization of the final species of complexes **1-3** in H_2O_2-disproportionation.

This study indicates that η^2-pyridazine and acac bridges are able to form a short Mn···Mn distance in the binuclear Mn^{II} complex and to mediate significant magnetic exchange interactions. We are, at variance with cases characterizing pyrimidine and pyrazine bridged manganese(II) behavior as having only a very weak antiferromagnetic chain.

ACKNOWLEDGEMENT

This work was supported by the National Science Council of Taiwan through Grant No. NSC-86-2113-M-032-005.

Received February 7, 1998.

Key Words

Crystal structure; Polynuclear complexes; Manganese complexes; Magnetic properties; Catalase activity.

REFERENCES

1. (a) Penner-Hahn, J. E. *Manganese Redox Enzymes*, ed. V. L. Pecoraro, VCH, New York, 1992; pp. 29-45. (b) Dismukes, G. C. *Chem. Rev.* **1996**, *96*, 2909-2926.
2. Dismukes, G. C. *Photochem. Photobiol.* **1986**, *42*, 187.
3. Barynin, V. V.; Vagin, A. A.; Melik-Adamyan, V. R.; Grebenko, A. I.; Khangulov, S. V.; Popov, A. N.; Andrianova, M. E.; Vainstein, B. K. *Dolk. Akad. Nauk. S. S. S. R.* **1986**, *228*, 877.
4. George, G.; Prione, R. C.; Cramer, S. P. *Science* **1989**, *243*, 789.
5. (a) Wieghardt, K. *Angew. Chem. Int. Ed. Engl.* **1989**, *28*, 1153. (b) Mathur, P.; Growder, M.; Mathur, G. C. *J. Am. Chem, Soc.* **1987**, *109*, 5227. (c) Sakiyama, H.; Okawa, H.; Suzuki, M. *J. Chem. Dalton Trans.* **1993**, 3829. (d) Pessiki, P. J.; Dismukes, G. C. *J. Am. Chem. Soc.* **1994**, *116*, 898. (e) Devereux, M.; McCann, M.; Casey, M. T.; Casey, M.; Ferguson, G. C.; Cardin, C.; Convery, M.; Quillet, V. *J. Chem. Soc. Dalton Trans.* **1995**, 771. (f) Quillet, C.; Sakiyama, H.; Okawa, H.; Fenton, D. E. *J. Chem. Soc. Dalton Trans.* **1995**, 4015. (g) Gelasco, A.; Pecoraro, V. L. *J. Am. Chem. Soc.* **1993**, *115*, 7928. (h) Gelasco, A.; Askenas, A.; Pecoraro, V. L. *Inorg. Chem.* **1996**, *35*, 1419.
6. (a) Steel, P. *Coord. Chem. Rev.* **1990**, *105*, 221; Thompson, L. K.; Tandon, S. S.; Manuel, M. E. *Inorg. Chem.* **1995**, *34*, 2356. (b) Masciocchi, N.; Cairati, P.; Carlucci, L.; Ciani, G.; Mezza, G.; Sironi, A. *J. Chem. Soc. Dalton Trans.* **1994**, 3009. (c) Otieno, T.; Rettig, S. J.; Thompson, R. C.; Trotter, J. *Inorg. Chem.* **1995**, *34*, 1718.
7. (a) Carlussi, L.; Ciani, G.; Moret, M.; Sironi, A. *J. Chem. Soc. Dalton Trans.* **1994**, 2397. (b) Brooker, S.; Kelly, R. J. *J. Chem. Soc. Dalton Trans.* **1996**, 2117.
8. Charles, R. G. *Inorg. Syn.* **1960**, *6*, 164.
9. Gate, E. J.; Le Page, Y.; Cherland, J. P.; Lee, F. L.; White, P. S. *J. Appl. Cryst.* **1989**, *22*, 384.
10. Kahn, O. *Molecular Magnetism*. VCH, New York, 1993.
11. Nakamoto, K. *Infrared and Raman Spectra of Inorganic and Coordination Compounds*, 5th edn. Wiely-Interscience, New York, 1996, Part B, p. 91.
12. Deguenon, D.; Bernardinelli, G.; Tuchagues, J. P.; Castan, P. *Inorg. Chem.* **1990**, *29*, 3031.
13. Menage, S.; Vitols, S. E.; Bergerat, P.; Codjovi, E.; Kahn, O.; Girerd, J. J.; Guillot, M.; Solans, X.; Calvet, T. *Inorg. Chem.* **1991**, *30*, 2666.
14. Struss, S. H.; Pawlik, M. J.; Skowyra, J.; Kennedy, J. R.; Anderson, O. P.; Spartalian, K.; Dye, J. L. *Inorg. Chem.* **1987**, *26*, 724.
15. Fisher, M. E. *Am. J. Phys.* **1964**, *32*, 343.
16. Mathur, P.; Crowder, M.; Dismukes, G. C. *J. Am. Chem. Soc.* **1987**, *109*, 5227.
17. (a) Owen, J. *J. Appl. Phys.* **1961**, *32*, 213S. (b) McPherson, G. L.; Chang, J. R. *Inorg. Chem.* **1976**, *15*, 1018.
18. (a) Larson, E. J.; Pecoraro, V. L. *J. Am. Chem. Soc.* **1991**, *113*, 3595. (b) Balasubramanian, P. N.; Schmidt, E. S.; Bruice, T. C. *J. Am. Chem. Soc.* **1987**, *109*, 7865.
19. Larson E. J.; Pecoraro, V. L. *J. Am. Chem. Soc.* **1991**, *113*, 3810.